



Letter

Dissociation of Ti_2O_3 from titania slag under mechanical activationGuo Chen^{a,b,*}, Jin Chen^{a,b}, Jinhui Peng^{a,b}, C. Srinivasakannan^c^a Key Laboratory of Unconventional Metallurgy, Ministry of Education, Kunming University of Science and Technology, Kunming 650093, PR China^b Faculty of Metallurgical and Energy Engineering, Kunming University of Science and Technology, Kunming 650093, PR China^c Chemical Engineering Program, The Petroleum Institute, P.O. Box 253, Abu Dhabi, United Arab Emirates

ARTICLE INFO

Article history:

Received 7 March 2011

Received in revised form 1 April 2011

Accepted 2 April 2011

Available online 9 April 2011

Keywords:

Titania slag

X-ray diffraction

Raman spectroscopy

Mechanical activation

Phase transformation

ABSTRACT

In this present study, the effects of mechanical activation on the characterization of titania slag were systematically investigated. The crystal structures, surface chemical functional groups, and microstructure of the samples were characterized before and after mechanical activation using XRD, FT-IR, and Raman spectroscopy techniques, respectively. It was found that untreated titania slag under mechanical activation was mainly composed of $\text{Fe}_3\text{Ti}_3\text{O}_{10}$ and rutile TiO_2 , but that of being treated by mechanical activation was mainly composed of $\text{Fe}_3\text{Ti}_3\text{O}_{10}$, Ti_2O_3 and rutile TiO_2 . Ti_2O_3 is transformed partially from $\text{Fe}_3\text{Ti}_3\text{O}_{10}$ under moderate mechanical activation conditions for 12 h. The demonstration of mechanical activation techniques can be applied effectively and efficiently to the treatment processing of titania slag.

Crown Copyright © 2011 Published by Elsevier B.V. All rights reserved.

1. Introduction

Titania slag is prepared from ilmenite ore by carbothermal reduction in an electric arc furnace [1–8]. In this process, a large fraction of the iron content of the ilmenite is reduced to metallic iron. The remainder of the materials is collected in a titania slag form [9–12]. The simultaneous reductions of the TiO_2 , Ti_2O_3 and FeO in the titania slag occur and their amounts are enriched [13]. The solidified slag are consists mainly of a single phase, which follows as the $\text{Fe}_3\text{Ti}_3\text{O}_{10}$ stoichiometry, and is often referred to as “anosovite” [14]. However, the oxidization of titania slag is found to be very slow under high temperature [15].

Mechanical activation is an important industrial operation that is used for the size reduction of materials, production of large surface area and liberation of valuable minerals from their matrices [16–19]. These results indicated that the mechanical activation process has advantages over conventional methods as the required roasting temperature is lower, reducing processing costs [20–25]. Thus, various physical and physico-chemical aspects of a mechanical activation operation have to be known [26–30].

Based on the concept mentioned above, the objective of this research was, on one hand, to study dissociation of titania slag through mechanical activation process using high performance

planetary mill, on the other hand, to characterize and analyze the titania slag and mechanically activated titania slag under different processing time, using X-ray diffraction (XRD), Fourier transform infrared radiation (FT-IR) and Raman spectroscopy.

2. Experimental

2.1. Materials

The raw material, titania slag, was obtained from Kunming city, Yunnan province, China. The chemical compositions of ilmenite were as follows (% (w/w)): TiO_2 , 72.33; Ti_2O_3 , 17.79; FeO, 5.26; MnO, 1.04; Al_2O_3 , 2.75; MgO, 2.30; SiO_2 , 2.57, respectively. It can be seen from Fig. 1 that $\text{Fe}_3\text{Ti}_3\text{O}_{10}$ (JCPDS card No. 43-1011) is mainly crystalline compounds in the titania slag. In addition, a minor amount of rutile TiO_2 (JCPDS card No. 65-0191) is present. The product was analyzed by the method in accordance with the recommended methods of National Standard of the People's Republic of China (GB/T).

2.2. Instrumentation

XRD instrument (D/Max 2200, Rigaku, Japan) was used to measure the crystal structure of the titania slag and the treated samples. XRD pattern was acquired using an X-ray diffractometer with $\text{Cu K}\alpha$ radiation and a Ni filter. The voltage and anode current operated were 35 kV and 20 mA, respectively. The continuously scanning rate with $0.25^\circ \text{ min}^{-1}$ of set time was used to record the XRD patterns of the samples.

The Raman studies were performed with a confocal microprobe Raman system (Renishaw Ramascope System 1000, UK). A 514-nm argon laser was used for excitation. Backscattered Raman signals were collected through a microscope and holographic notch filters in the range of $100\text{--}1000 \text{ cm}^{-1}$ with a spectral resolution of 2 cm^{-1} . The laser power on the sample surface was $20 \mu\text{W}$, the spot diameter was $5 \mu\text{m}$ and the typical collection time of one measurement was 10 min.

The infrared spectra of the titania slag before and after mechanical activation were collected using FT-IR spectrometer equipped (8700, Nicolet, USA). The angle of incidence of the IR beam was 45° and 100 scans were collected at a resolution of

* Corresponding author at: Key Laboratory of Unconventional Metallurgy, Ministry of Education, Kunming University of Science and Technology, Kunming 650093, PR China. Tel.: +86 871 5192076; fax: +86 871 5191046.

E-mail address: realchenguo@yahoo.com.cn (G. Chen).

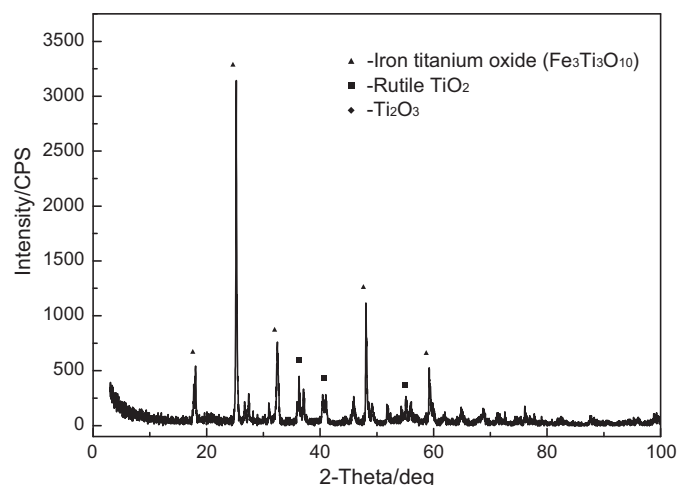


Fig. 1. XRD pattern of raw materials.

4 cm^{-1} and averaged using the OMNIC spectroscopic software. The spectral range was $4000\text{--}400\text{ cm}^{-1}$.

A planetary mill (QM-3SP2, Nanjing, China) was employed for the mechanical activation of titania slag. The milling cells were 400 ml agate jar filled with 100 g agate balls of 10 mm in diameter and 150 g agate balls of 6 mm in diameter. No other additives were used during the mechanical activation process. After completion of the milling operation, the contents of the agate jar and the agate balls were thoroughly cleaned and dried before the next mechanical activation experiment. The particle size analysis was carried out using a laser diffraction analyzer (Mastersize2000, Malvern, UK).

2.3. Procedure

Prior to the use, titania slag was loaded on a ceramics boat which was placed inside a stainless steel tubular reactor. Then the samples were heated to 393 K at a heating rate of 278 K/min in the drying oven and held at this temperature for 120 min. After drying, the samples were cooled to room temperature. The total mass of sample taken was 25 g for each experimental run.

3. Results and discussion

The particle size distributions of the titania slag and mechanically activated titania slag for various times are illustrated in Fig. 2. The original titania slag is composed of the particles with a d_{50} around $120\text{ }\mu\text{m}$, in which about 70% of the particles are below $100\text{ }\mu\text{m}$. It could be seen that after 12 h of mechanical activation, the d_{50} decreased from $110\text{ }\mu\text{m}$ to $5.8\text{ }\mu\text{m}$. And then, longer mechani-

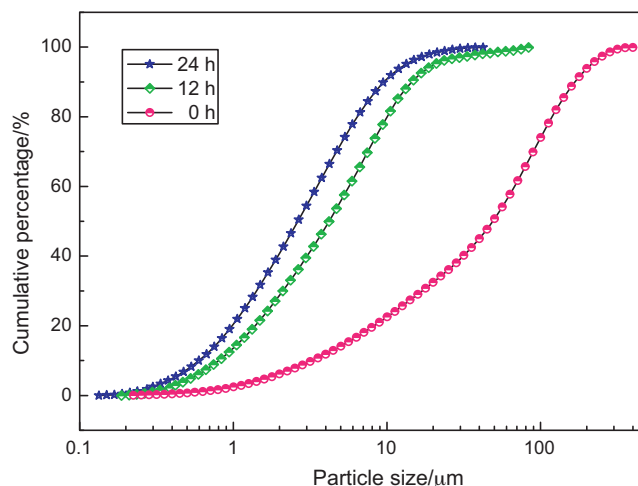


Fig. 2. Particle size distributions of the titania slag before and after mechanical activation for different times.

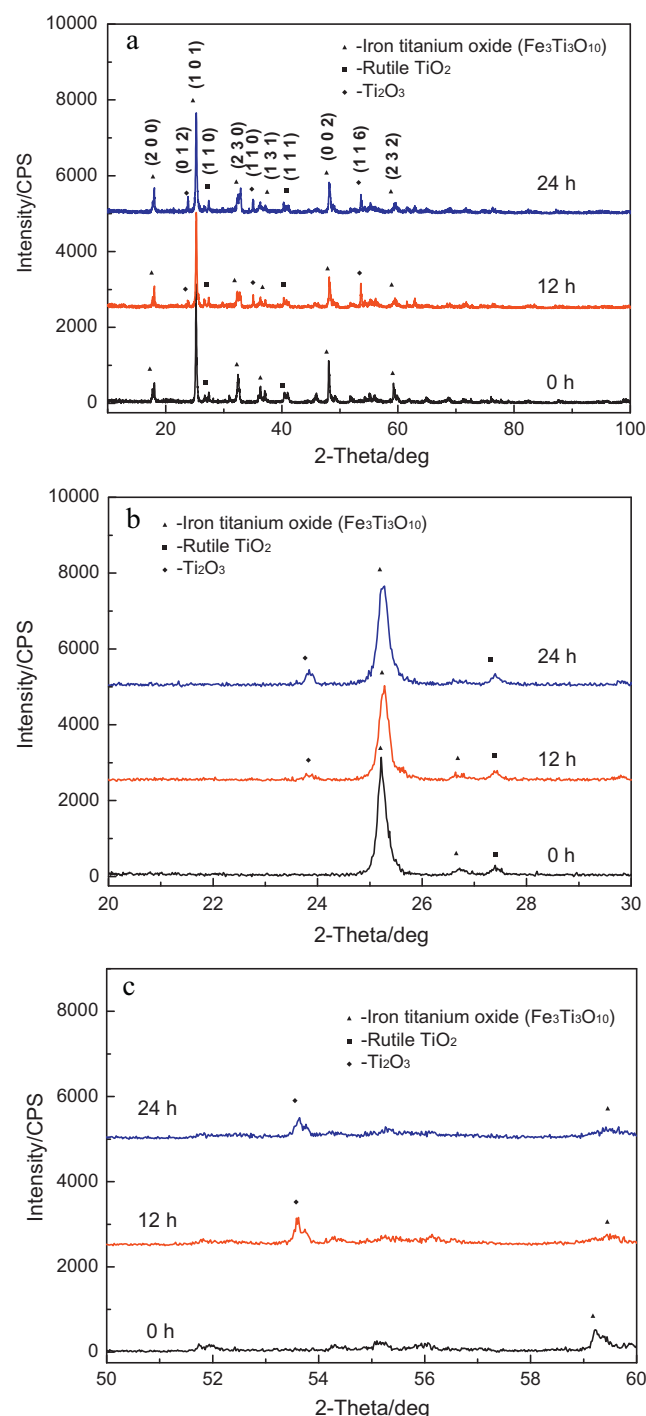


Fig. 3. X-ray diffraction patterns of titania slag before and after mechanical activation. (a) The 2θ range of $3\text{--}100^\circ$, (b) the 2θ range of $20\text{--}30^\circ$, and (c) the 2θ range of $50\text{--}60^\circ$.

cal activation times up to 24 h essentially had a minor effect on the distribution. The d_{50} slowly decreased to $3.5\text{ }\mu\text{m}$.

The titania slag before and after mechanical activation is characterized by XRD and the results are illustrated in Fig. 3, respectively. Compared with raw materials, the strong preferential orientation of (116) and (110) planes of the mechanically activated titania slag were observed, where the strongest and the second strongest peaks of Ti_2O_3 phase (JCPDS card No. 43-1033) occur, respectively [31]. The third strongest at orientation (012) peak, remained and it, however, significantly and asymmetrically broadened [32]. It can

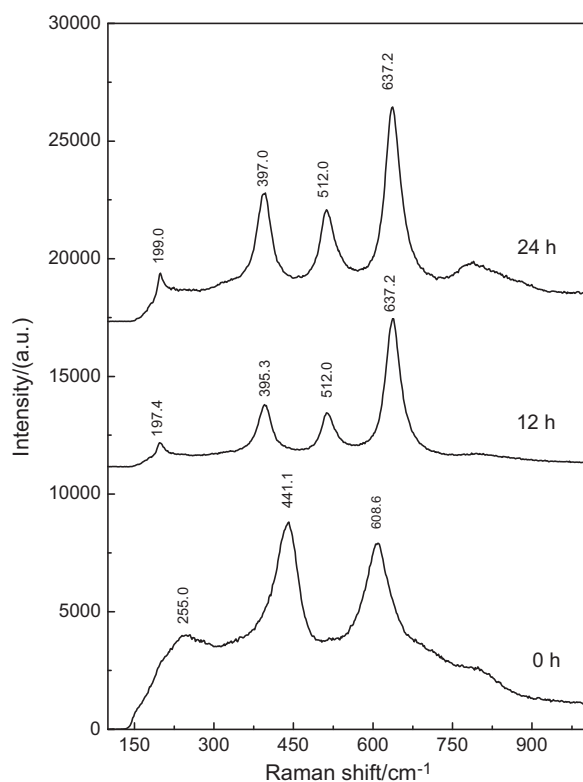


Fig. 4. Raman spectra of titania slag before and after mechanical activation.

be inferred from XRD data that $\text{Fe}_3\text{Ti}_3\text{O}_{10}$ is partially disintegrated to Ti_2O_3 . And it is known that the Ti_2O_3 can be oxidized more easily than iron titanium oxide. The resulting mechanically activated titania slag can be better used for the production of synthetic rutile.

The typical Raman spectra of the different mechanical activation time are presented in Fig. 4. In all spectra the presence of Raman shifts of titania slag at 255.0, 441.1 and 608.6 cm^{-1} are clearly identified. An increase of intensity of the band at $\sim 197.4\text{ cm}^{-1}$ in Raman spectra of mechanically activated titania slag occurs under 12 h. Intensity of the former band originated from vibrations of Ti–O bonds in Ti_2O_3 structure increases only slightly [33]. With increasing mechanical activation time, the amount of phase crystallized in the form of Ti_2O_3 also increases, which is confirmed by an appearance of its band with a low intensity located at $\sim 199.0\text{ cm}^{-1}$ [34]. It implies that at this mechanical activation process, iron titanium oxide can be partially transformed into Ti_2O_3 in samples with different mechanical activation time. The broadness of these bands suggests low chemical composition of Ti_2O_3 .

The surface chemical functional groups of the samples were characterized before and after mechanical activation using FT-IR and the results are shown in Fig. 5. The FT-IR absorption was showed a broad band at ~ 3434.2 and $\sim 1067.1\text{ cm}^{-1}$ due to the stretching vibrations of O–H bonds, Peaks at $\sim 1641.2\text{ cm}^{-1}$ due to the H–O–H bending vibrations of interlayer adsorbed H_2O molecule at the minerals surface, respectively. The weak band 2350 cm^{-1} is considered to come from the adsorbed atmospheric CO_2 at titania slag surface. In the range of $400\text{--}1000\text{ cm}^{-1}$, the IR bands of inorganic solids are usually assigned to the vibration of metallic ions in the crystal lattice. Peaks at $\sim 493.3\text{ cm}^{-1}$ due to the stretching vibrations of Ti–O and Ti–O–Ti of the TiO_2 units. It could be seen from Fig. 4 that the bands at 465.3 cm^{-1} of untreated titania slag gradually disappeared and significantly shifted toward low-wave number after mechanical

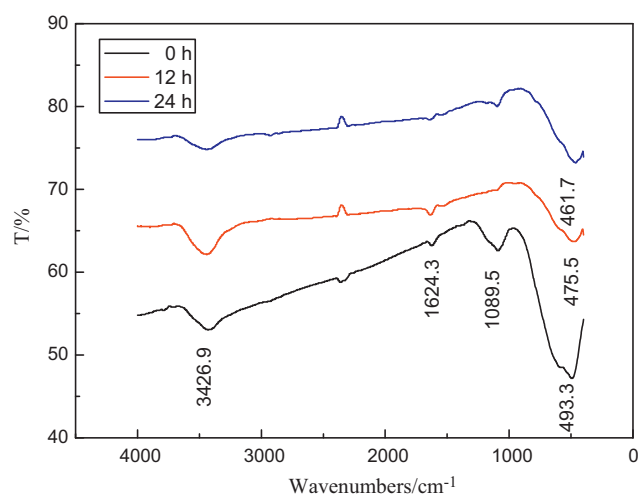


Fig. 5. FT-IR of titania slag before and after mechanical activation.

activation, indicating considerable variations in the mineral crystal structure.

4. Conclusion

Experiments were carried out to study on dissociation of titania slag under mechanical activation using high performance planetary mill. Ti_2O_3 was successfully disintegrated from $\text{Fe}_3\text{Ti}_3\text{O}_{10}$ of titania slag through a new route. The XRD, FT-IR and Raman spectroscopy techniques have proved helpful in the investigation to explain the occurred transformations and it is recommended that they should also be used in the future work. The results demonstrate that the mechanical activation can take the place of the traditional high temperature pretreatment of titania slag.

Acknowledgements

The authors thank Prof. S.M. Wen, Prof. H.X. Dai, Prof. Y.X. Hua and Prof. L.B. Zhang for stimulating discussions. Financial supports from the National Basic Research Program of China, grant no. 2007CB613606, and the National Natural Science Foundation of China, grant nos. 51090385, 50734007, and 50974067.

References

- [1] S. Samal, B.K. Mohapatra, P.S. Mukherjee, S.K. Chatterjee, *J. Alloys Compd.* 474 (2009) 484.
- [2] C. Li, B. Liang, *J. Alloys Compd.* 459 (2008) 354.
- [3] G. Chen, J.H. Peng, J. Chen, S.M. Zhang, *High Temp. Mater. Process.* 28 (2009) 165.
- [4] Y. Chen, M. Marsh, J.S. Williams, B. Ninham, *J. Alloys Compd.* 245 (1996) 54.
- [5] C.S. Kucukkaragoz, R.H. Eric, *Miner. Eng.* 19 (2006) 334.
- [6] G. Chen, J. Chen, J.H. Peng, R.D. Wang, *Trans. Nonferrous Met. Soc. China* 20 (2010) s198.
- [7] M. Klepka, K. Lawniczka-Jablonska, M. Jablonski, A. Wolska, R. Minikayev, W. Paszkowicz, A. Przepiera, Z. Spolnik, R. Van Grieken, *J. Alloys Compd.* 401 (2005) 281.
- [8] T.A.I. Lasheen, *Hydrometallurgy* 76 (2005) 123.
- [9] G. Chen, K. Xiong, J.H. Peng, J. Chen, *Adv. Powder Technol.* 21 (2010) 331.
- [10] N. Setoudeh, A. Saidi, N.J. Welham, *J. Alloys Compd.* 390 (2005) 138.
- [11] D. Bessinger, J.M.A. Geldenhuis, P.C. Pistorius, A. Mulaba, G. Hearne, *J. Non-Cryst. Solids* 282 (2001) 132.
- [12] W. Mo, G.Z. Deng, *Titanium Metallurgy*, Publishing Press of Metallurgical Industry, Beijing, 1998.
- [13] P.C. Pistorius, T. Mottham, *Miner. Eng.* 19 (2006) 232.
- [14] J. Yu, Y. Chen, *J. Alloys Compd.* 504 (2010) S364.
- [15] N. Setoudeh, A. Saidi, N.J. Welham, *J. Alloys Compd.* 395 (2005) 141.
- [16] C. Sasikumar, D.S. Rao, S. Srikanth, B. Ravikumar, *Hydrometallurgy* 75 (2004) 189.
- [17] Y. Chen, J.S. Williams, S.J. Campbell, G.M. Wang, *Mater. Sci. Eng. A* 271 (1999) 485.

- [18] Z.Q. Huang, J.P. Lu, X.H. Li, Z.F. Tong, Carbohydr. Polym. 68 (2007) 128.
- [19] N.J. Welham, J. Alloys Compd. 274 (1998) 260.
- [20] K. Fukui, K. Kanayama, T. Yamamoto, H. Yoshida, Adv. Powder Technol. 18 (2007) 805.
- [21] J. Temuujin, R.P. Williams, A. van Riessen, J. Mater. Process. Technol. 209 (2009) 5276.
- [22] D. Feng, C. Aldrich, Int. J. Miner. Process. 60 (2000) 115.
- [23] B.B. Bokhonov, I.G. Konstanchuk, V.V. Boldyrev, Mater. Res. Bull. 30 (1995) 1277.
- [24] A. Ozkan, M. Yekeler, M. Calkaya, Int. J. Miner. Process. 90 (2009) 67.
- [25] G. Chen, J.H. Peng, J. Chen, Miner. Metall. Process. 28 (2011) 44.
- [26] K. Fukui, M. Katoh, T. Yamamoto, H. Yoshida, Adv. Powder Technol. 20 (2009) 35.
- [27] F. Garcia, N. Le Bolay, C. Frances, Chem. Eng. J. 85 (2002) 177.
- [28] R.A. Kleiv, M. Thornhill, Miner. Eng. 19 (2006) 340.
- [29] C. Li, B. Liang, S.P. Chen, Hydrometallurgy 82 (2006) 93.
- [30] C. Li, B. Liang, L.H. Guo, Z.B. Wu, Miner. Eng. 19 (2006) 1430.
- [31] M.A. Afifi, M.M. Abdel-Aziz, I.S. Yahia, M. Fadel, L.A. Wahab, J. Alloys Compd. 455 (2008) 92.
- [32] Z. Lin, K. Liu, Y.C. Zhang, X.J. Yue, G.Q. Song, D.C. Ba, Mater. Sci. Eng. B: Solid State Mater. Adv. Technol. 156 (2009) 79.
- [33] S.J. Bae, U. Kang, O. Dymshits, A. Shashkin, M. Tsenter, A. Zhilin, J. Non-Cryst. Solids 351 (2005) 3969.
- [34] P. Xiao, S.B. Zheng, J.L. You, Spectrosc. Spectr. Anal. 5 (2007) 936.